ANALYSIS AND OPTIMIZATION OF CYCLONE
SEPARATORS BY USING RANS

Matheskankanamge Shashi Manoj De Silva

(119253H)

Dissertation submitted in partial fulfillment of the requirements for the degree Master
of Science in Sustainable Process Development
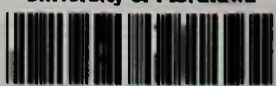
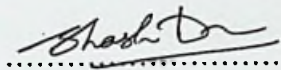Department of Chemical and Process Engineering

University of Moratuwa

Sri Lanka

January 2016

DECLARATION OF THE CANDIDATE & SUPERVISOR

"I declare that this is my own work and this thesis does not incorporate without acknowledgement any material previously submitted for a Degree or Diploma in any other University or institute of higher learning and to the best of my knowledge and belief it does not contain any material previously published or written by another person except where the acknowledgement is made in the text.

Also, I hereby grant to University of Moratuwa the non-exclusive right to reproduce and distribute my thesis, in whole or in part in print, electronic or other medium. I retain the right to use this content in whole or part in future works."

2016. 10 .10

Signature: Date:

The above candidate has carried out research for the Master Dissertation under my supervision.

UOM Verified Signature

2016 . 10 . 10

Signature of the supervisor   Date:

Dr. Mahinsasa Narayana

Senior Lecturer Grade II

i

ABSTRACT

Many types of particulate matter collectors are used in the industry to separate particulate matter from the gaseous streams. Among various type of particulate collectors, cyclone separators are one of the most extensively used gas cleaning equipment because of they are inexpensive; easier to fabricate, and could be designed to stand under harsh operating conditions.

Due to this extensive usage in the industry, many theoretical and experimental studies have been carried out and empirical models were developed to predict cyclone separator's most important operational parameters. These models have many limitations of illustrating flow behavior properly due to the complex nature of the cyclone gas–solid flow behavior. Computational Fluid Dynamic (CFD) simulation could be useful to predict cyclone performance as an alternative approach.

This work represents a CFD simulation of a Lapple cyclone separator using OpenFOAM software. Cyclone simulations have been carried out using turbulence models associated with the Reynolds Average Navier Stokes (RANS) equations. Multiphase Particle in Cell (MPPIC) method was used for the particle modeling, in which particle interactions with other particles were represented by models. The perditions of simulations have been compared both mutually and to literature in terms of cyclone pressure drop, gas-solid flow pattern and collection efficiency.

RANS model fairly predict the gas-solid flow pattern of the cyclone. Pressure drop and collection efficiency of cyclone well fitted to the experimental results in the literature.

Optimum values for inlet gas-solid velocity and particulate loading rate for the Lapple cyclone were obtained by RANS analysis. Pressure drop variation with gas-solid inlet velocity which has been obtained by this analysis could be useful to minimize the energy requirement while maintaining the required collection efficiency.

ACKNOWLEDGMENT

I would like to express my heartiest gratitude to my research supervisor Dr. M. Narayana, a Senior Lecturer of Department of Chemical and Process Engineering of University of Moratuwa, for his enormous encouragement, guidance, dedication and patience throughout the research to make it successful.

My sincere thanks also go to Dr. A Rathnasiri, Head of the Department - Department of Chemical and Process Engineering of University of Moratuwa, for teaching Computational Fluid Dynamics in interesting manner and giving essential basic theoretical background of CFD.

I would like to thank to Dr. S Amarsinghe a Senior Lecturer of Department of Chemical and Process Engineering of University of Moratuwa, for teaching theoretical background of fluid dynamics and encouraging on research work.

My special thanks go to Mr.Suren Watson, Environmental Manager of SGS Lanka (Pvt) Ltd. for encouraging me to select the field of pollution control equipment as my research and for his enormous support given throughout the research to fulfill this work successfully.

I would like to thank IT staff members and non-technical staff members for the support given by providing lab facilities.

My heartiest thanks also go to my loving wife; D. Jayani Chathurika since without the help and support of her, this research could not be completed in to this success.

TABLE OF CONTENTS

LIST OF FIGURES

LIST OF TABLES

LIST OF ABBREVATIONS

Abbreviation	Description
β	constants
δ_{ij}	Kronecker delta
Δ	lattice spacing constant
ΔP	static pressure drop
Δt	residence time of gas
θ_{cp}	close pack volume fraction
λ_{mix}	mixing length of the sub grid scale
μ	viscosity of gas
μ_t	eddy (turbulent) viscosity
ν_e	eddy viscosity
ε	dissipation of turbulent kinetic energy
ρ	density
ρ_g	density of gas
ρ_g	density of gas
ρ_p	density of particle
τ	particle stress
φ	a property of a flow
Φ	the mean property
Ω_p	particle volume at position x and time t
ω_k	rotational vector
A	particle acceleration
B_c	cyclone inlet width
C_μ	dimensionless constant
C_s	a constant
D_p	diameter of the particle
D, D_c	diameter of the cyclone

D_e	diameter of gas exit
d_p	diameter of the particle
d_{pc}	diameter of the particle collected with 50% efficiency
F	Particle phase and gas phase momentum exchange rate
H_c	cyclone inlet height
H_c	cyclone inlet height
H_v	the pressure drop, which is given in terms of number of inlet velocity heads
J_c	diameter of dust outlet
K	constant, function of cyclone design and operating parameters
k	turbulent kinetic energy
L_c	height of cylindrical section
L_c	length of cylindrical body
N_e	number of effective revolutions in the outer vortex
n	vortex exponent
n_1	vortex component at 283K
n_2	vortex component operating temperature
P	total pressure in the cyclone
P_s	constant
R	radius of the cyclone body
R_{ij}	Reynolds stress ($u_i' u_j'$)
r	radial distance from center axis (m)
S_c	length of vortex finder from inlet width
S^2	squared resolved deformation rate
T_1	283K
T_2	operating temperature
U	mean velocity of flow
U_x	tangential gas velocity
U_y	radial gas velocity

U_z	axial gas velocity
u	three dimensional velocities
u'	instantaneous fluctuating velocity component
u_p	particle velocity
V_i	gas inlet velocity
V_{ct}	tangential gas velocity component (m/s)
Vt	terminal velocity
Z_c	height of conical section
Z_c	length of cone

LIST OF APPENDICES

1 INTRODUCTION

Cyclone separators are one of the most extensively used gas cleaning equipment in the process industry. The main reasons for the wide spread use of cyclone separators are that they are inexpensive; easier to fabricate, and could be designed to stand under harsh operating conditions. Cyclones utilize centrifugal forces and inertia to separate solid or liquid particles from a carrier gas. It yields fast separation and requires less space over slow gravity settling chambers.

Particle removal efficiency of cyclone greatly varies with many operational and geometrical parameters. The most important performance variables are usually gas pressure drop and solid separation efficiency. Flow and particle behavior inside the cyclone is complex and not possible to be fully understood using measuring techniques.

Swirling flow and particulate behavior of cyclones could be reasonably visualized using Computational Fluid Dynamic (CFD) model. Furthermore, this understanding is useful to optimize the cyclone design for industrial applications. Advancement of computer processing power and memory capacity during last two decades made discover of fluid flow behavior by means of CFD more effective and easier. This was an initiation of new chapter of studding fluid flow behavior. Cost effective full scale dynamic fluid flow pattern could be obtained using CFD, which is not possible to obtain from inexpensive measuring technologies.

Most of the researches have been based on commercially available expensive software packages. In this work, open source software package "OpenFOAM" was used to study the gas–solid flow in a typical Lapple cyclone separator.

Cyclone simulations have been arranged using turbulence models associated with the Reynolds Average Navier Stokes (RANS) equations. The simulations results were compared mutually and with experimental data in literature in terms of cyclone pressure drop, gas-solid flow pattern and collection efficiency.

2 LITERATURE SURVEY

2.1 Overview of Particulate Collectors

Many types of particulate matter collectors are used in the industry to separate particulate matter from the gaseous streams, utilizing various technologies for the purpose. Wet scrubbers, cyclone separators, gravity settling chambers, bag filters, electro static precipitators and venturi scrubbers are common types of widely used particle separators. Size range of collected particles and form of collection varies with the collection technology. Therefore, most suitable type of particulate collector should be selected and designed according to the case by case.

Most commonly used process industrial applications of collectors are separating particulate product from the gas solid mixture, purifying the exhaust emissions from particulate generating applications, recovering product from spray drying, recovering catalyst after reactions, and cleaning of process streams before release into the environment.

Table 2.1 : Overview of particulate collectors

Type of equipment	Minimum particle size (μm)	Approx. efficiency (%)	Typical gas velocity (m/s)	Gas pressure drop (mm H_2O)
Dry collectors				
Settling chamber	50	50	1.5-3	5
Baffle chamber	50	50	5-10	3-12
Louver	20	80	10-20	10-15
Cyclone	10	85	10-20	10-70
Multiple cyclone	5	95	10-20	50-150
Impingement	10	90	15-30	25-50
Wet collectors				
Gravity spray	10	70	0.5-1	25
Centrifugal	5	90	10-20	50-100
Impingement	5	95	15-30	50-200
Packed	5	90	0.5-1	25-250
Jet	0.5 to 5	90	10-100	none
Venturi	0.5	99	50-200	250-750
others				
Fabric filters	0.2	99	0.01-0.1	50-150
Electrostatic precipitators	2	99	5-30	5-25

Source: Coulson and Richardson [1]

Among these separators, cyclone is enormously popular in industrial applications due to its geometrical simplicity, low fabrication cost and low maintenance cost.

2.2   Cyclone Separator

2.2.1   Principals of cyclonic separation

Cyclones, centrifugal separators, inertial separators and cyclone collectors are different terms to identify cyclone separator in the industry. A cyclone is basically a conical shape settling chamber, which utilizes centrifugal forces and inertia to separate particles from the gas stream. Gas-solid flow enters the cyclone through the tangential inlet, where the flow is forced into a cyclic movement down the cyclone. At the cyclone bottom, gas turns upward and spiral up around the center axis and exit through the vortex finder [10]. An impression of the gas flow in the cyclone is shown in Figure 2.1.
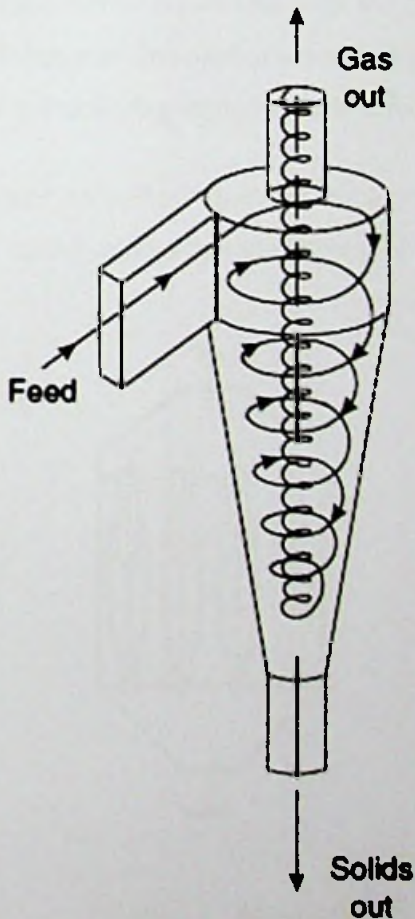
Figure 2.1 : Flow pattern of the reverse-flow cyclone

Source: Coulson and Richardson [1]

While the gas-solid flow travels inside the outer vortex, solid particles start to settle. Firstly, heavy particles easily move towards the cyclone wall due to the inertia and then they travel down to the dust collector bin. Then the medium size particles move towards the wall at terminal velocity. Centrifugal force acting on medium size particle is higher than the drag force. These particles should be reached the wall within the gas residence time on outer vortex, to be collected. All other fine particles escape through the gas outlet, as centrifugal forces and gravity forces on fine particles are not sufficient to overcome drag forces acting on them [2].

Separation force in the cyclone may vary from 5 to 2500 times gravity depending on its design [3]. Considering the classic cyclones, separation is limited to large particles and they are not suitable to remove particles with the diameter less than 5 μm [3]. However collection efficiency of fine particulate matter could be improved further by design improvements and employing agglomeration effect [3].

Multi-cyclone is designed to collect fine particulate matter at higher efficiency, which contains a set of mini-cyclones operate in parallel.
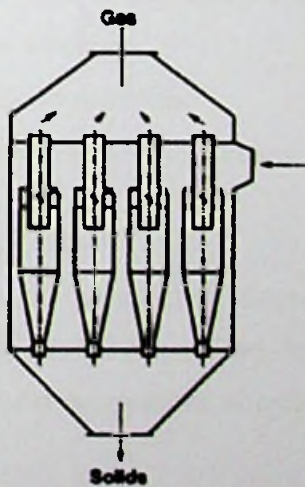
Figure 2.2 : Multicyclone

Source: Perry and Green [3]

2.2.2   Advantages and disadvantages of cyclone separators

Compared to the other separation devises, advantages of cyclone separators are as follows [2].

- low capital investment
- low maintenance requirements because there are no moving parts
- collected product remains dry
- space requirement is relatively small
- could be constructed from easily available materials such as plate steel, casting metals, alloys, aluminum, plastics, ceramics, etc.
- could be used for both solid and liquid particulates
- could be used for any harsh conditions such as high temperature, high pressure and chemically abrasive conditions.

Disadvantages of cyclone separator over other separation devices are listed below.

- low efficiency for particles below the cut point diameter under low solid loading
- cyclone separators are not sufficient to meet environmental regulations
- not effective to remove low density fine particles
- pressure drop thorough the flow is high compared to other separators including bag filters and low pressure scrubbers
- unable to handle sticky or tacky materials
- high efficiency units may experience high pressure drops

2.2.3   Typical industrial applications

The industrial cyclone has a unique position among various types of gas-solid separators. Moreover, cyclones could be utilized for solid-liquid separation and liquid-liquid separation. Industrial applications of cyclone separators could be listed as follows.

- purification of process streams before release into the environment
- recovering of catalyst form the fluid catalyst cracking process in oil and gas industry
- recovering of particles in the fluidized bed reactors

- recovering of product from spray drying
- using as a pre cleaner when final cleaning is expensive. Eg. Bag filters, Electro static precipitators
- recovering of product from grinding, crushing and calcining process
- collecting of wood dust from sawing
- separating of sludge from treated waste water

2.3   Cyclone Gas Solid Flow Behavior and Collection Efficiency

2.3.1   Tangential gas velocity

The gas stream, which foams a vortex such that tangential gas velocity component (V_{ct}) increases with reducing radial distance (r) from wall to vortex finder radius. Ter Linden [4] had obtained an empirical equation for tangential velocity of a cyclone.

$$V_{ct} \sim r^{-n} \tag{2.1}$$

Where,

V_{ct} = Tangential gas velocity component (m/s)

n = vortex exponent

r = radial distance from center axis (m)

The tangential gas velocities of some regions of cyclone may reach to a higher value than inlet gas velocity.

At the absence of wall friction, ideally 'n' should be equal to 1 for free vortex and (−1) for forced vortex [3]. From the measurements where performed by Shepherd and Lapple [5]. It was found that magnitude of 'n' is varying from 0.5 to 0.7 over a large section of cyclone radius.

Ter Linden [4] has proposed a value for vortex component (n), which was proved to be accurate even in later studies with advance measuring techniques [6]. He proposed that the magnitude of n should be 0.52 for the vortex component. Further he stated that could be applicable only for the section, starting from the radius of vortex finder to the cyclone wall. However the tangential gas velocity approaches zero at the wall due to wall friction.
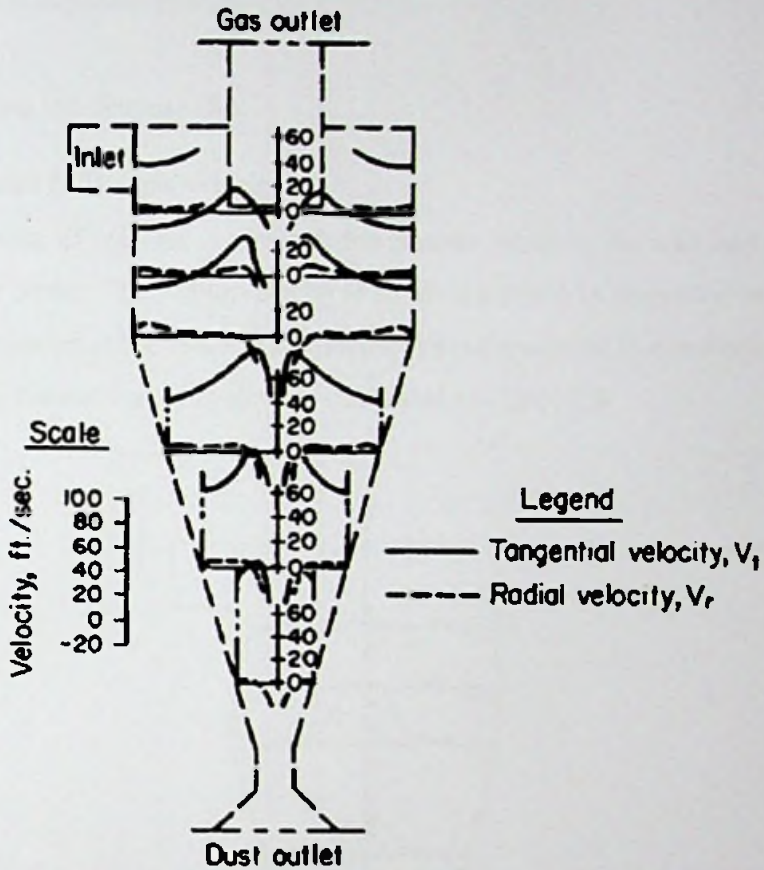
Figure 2.3 : Variation of tangential gas velocity and radial velocity in the cyclone

Source: Ter Linden [4]

An empirical expression for the vortex finder in a cyclone with the diameter D at temperature of 283K developed by Alexander [7] is given below.

$$n = 0.67D^{0.14} \hspace{3cm} (2.2)$$

Where,

D = diameter of cyclone, m

Temperature correction to the vortex component is expressed as;

$$\frac{1-n_1}{1-n_2} = \left(\frac{T1}{T2}\right)^{0.2} \hspace{3cm} (2.3)$$

Where,

n_1 = vortex component at 283K

n_2 = vortex component operating temperature

T_1= 283K

T_2 =operating temperature (K)

2.3.2 Axial and radial gas velocity

The axial velocity of cyclone is directed downwards closer to the wall and directed upwards at the center. The radial velocity is small compared to tangential velocities. It is directed outward at the center and directed toward center all over other areas [3]. Radial velocity distribution of cyclone is illustrated in Figure 2.4.
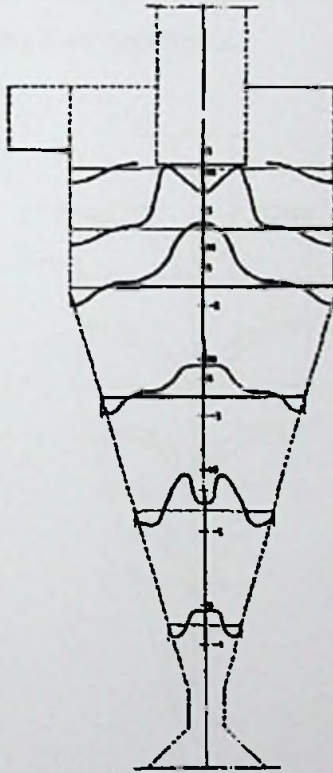
Figure 2.4 : Variation of axial velocity component in the cyclone

Source: Ter Linden [4]

2.3.3 Pressure distribution

Considering the cyclone, total pressure is sum of the static and velocity pressure. Total pressure becomes high at the cyclone wall and it gradually reduces towards the

center. Applying 'Navior-Stokes' equation in the radial direction with assuming steady state flow, it can be simplified to obtain following expression.

$$\frac{\partial P}{\partial r} = \rho_g \frac{V_{ct}^2}{r} \qquad (2.4)$$

Where,
   P = total pressure
   ρ_g = density of gas
   r = radial distance from center axis

Static pressure along the center line of the cyclone may drop below the atmospheric pressure due to strong swirling flow conditions.
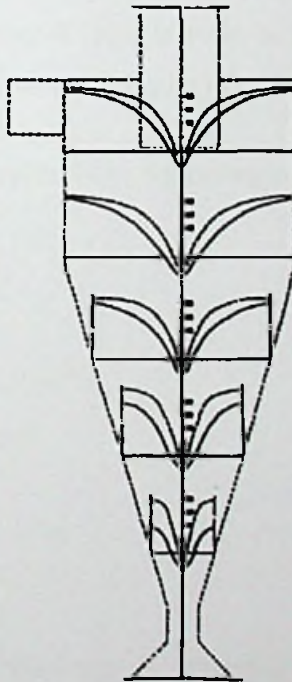
Figure 2.5 : Static pressure (-) and Total pressure (--) variation through the cyclone

Source: Ter Linden [4]

2.3.4   Pressure drop

Pressure drop of cyclone separator is a major concern, because that is directly related to the energy consumption. Generally higher efficiencies can be obtained by increasing the pressure drop through the cyclone with the cost of higher energy

consumption. Therefore, proper balance between collection efficiency of particles and running cost of the system generate an economical design.

There are several approaches to calculate pressure drop through the cyclone. Shepherd and Lapple approach is easy to use compared to advanced methods and it gives accurate results [2].

Shepherd and Lapple method [5],

$$H_v = K \frac{ab}{D_e^2} \qquad (2.5)$$

Where,

H_v = the pressure drop, which is given in terms of number of inlet velocity heads

K = constant, a function of cyclone design and operating parameters

Ideally K can fluctuate; however K value is set to be 16 for a cyclone that is used as a dust separator with a standard tangential inlet [8].

Static pressure drop can be expressed by following equation.

$$\Delta P = \frac{1}{2} \rho_g V_i^2 H_v \qquad (2.6)$$

Where,

ΔP = static pressure drop (N/m^2)

V_i = gas inlet velocity (m/s)

ρ_g = gas density (kg/m^3)

2.3.5 Collection efficiency

Overall particle collection efficiency is generally described as percentage mass fraction collected by the cyclone. Since this value is related to the particle size distribution, fractional collection efficiency (η) is used to define cyclone collection efficiency. The fractional efficiency is; mass fraction percentage collected compare to injected mass of particles with same size.

Many research studies have been carried out to develop models and empirical equations to predict particle collection efficiency of cyclone. These research and

experiments show wide verity with respect to operating conditions such as temperature, pressure, inlet gas flow rate, and mass injection rate [6].

Particles which enter to the cyclone are subjected to centrifugal forces. Large particles will reach cyclone wall quickly, due to its inertia. However other particles move towards the down with the gas flow under the forces such as centrifugal force, drag force and gravity. They will reach to terminal velocity (V_t) when opposing drag forces equal to the centrifugal forces. Particle should reach cyclone wall at a time period which is less than residence time of gas in outer vortex to be collected.

Residence time of gas in the outer vortex can be given by following equations.

$$\Delta t = \frac{2\pi DN_e}{V_t} \qquad (2.7)$$

Where,

Δt = residence time of gas (s)

N_e = number of effective revolutions in the outer vortex

$$N_e = \frac{1}{H_c}\left[Z_c + \frac{L_c}{2}\right] \qquad (2.8)$$

Where,

H_c = inlet height (m)

Z_c = height of conical section (m)

L_c = height of cylindrical section (m)

Terminal velocity that will just allow particle to be collected in time Δt could be written as follows.

$$V_t = \frac{B_c}{\Delta t} \qquad (2.9)$$

Where,

V_t = terminal velocity (m/s)

B_c = cyclone inlet width (m)

Assuming stokes regime flow and sphere particles, Terminal velocity could be expressed as follows.

$$V_t = \frac{d_p^2(\rho_p - \rho_g)V_i^2}{18\mu R}$$ (2.10)

Where,

d_p = diameter of the particle (m)

R = radius of the cyclone body (m)

ρ_g = density of gas (kg/m³)

ρ_p = density of particle (kg/m³)

μ = viscosity of gas (kg/ms)

Substituting of equation 2.9 into 2.10 and eliminating terminal velocity term, we can obtain an equation for the smallest particle size (d_p), which will be 100% collected in the cyclone.

$$d_p = \left[\frac{9\mu B_c}{\pi N_e V_i (\rho_p - \rho_g)}\right]^{1/2}$$ (2.11)

Lapple (1940) has proposed a semi empirical equation to find out 50% cut diameter. It is given by;

$$d_{pc} = \left[\frac{9\mu B_c}{2\pi N_e V_i (\rho_p - \rho_g)}\right]^{1/2}$$ (2.12)

Where,

d_{pc} = diameter of the particle collected with 50% efficiency (m)

2.4 Design of Cyclone

2.4.1 Standard designs

In the literature, five commonly used cyclone separators designs can be found. There dimensions of inlet, vortex finder, cone height, cone tip diameter and cylindrical body height given as fractions of cylindrical body diameter. Following table summarizes commonly used cyclone designs in the industry.

Table 2.2 : Standard cyclone dimensions

Cyclone type	High efficiency		Conventional		High throughput	
Adapted by	Stairmand (1951)	Swift (1939)	Lapple (1951)	Swift (1939)	Stairmand (1951)	Swift (1939)
Diameter of body, D/D	1.0	1.0	1.0	1.0	1.0	1.0
Height of inlet, H_c/D	0.5	0.44	0.5	0.5	0.75	0.8
Width of inlet, B_c/D	0.2	0.21	0.25	0.25	0.375	0.35
Diameter of gas exit, D_e/D	0.5	0.4	0.5	0.5	0.75	0.75
Length of vortex finder, $(H_c + S_c)$ /D	0.5	0.5	0.625	0.6	0.875	0.85
Length of cylindrical body, L_c/D	1.5	1.4	2.0	1.75	1.5	1.7
Length of cone, Z_c/D	2.5	2.5	2.0	2.0	2.5	2.0
Diameter of dust outlet, J_c/D	0.375	0.4	0.25	0.4	0.375	0.4

$B_c = D_c/4$
$D_e = D_c/2$
$H_c = D_c/2$
$L_c = 2D_c$
$S_c = D_c/8$
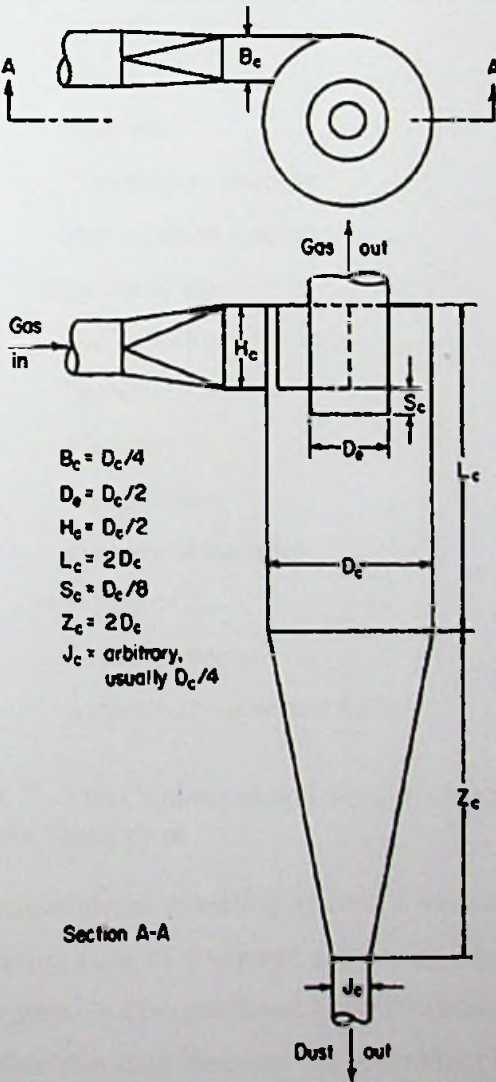$Z_c = 2D_c$
$J_c =$ arbitrory, usually $D_c/4$

Section A-A

Figure 2.6 : Lapple cyclone separator proportions

Source : Perry and Green [3]

2.4.2 Factors affecting the cyclone performance

There are numerous factors that affect the cyclone performance. They could be mainly categorized into four sections as given below [9].

- Cyclone dimensions
  - Cyclone diameter
  - Inlet height and inlet width
  - diameter and length of vortex finder
  - height of cylindrical section
  - height of conical section
  - diameter of the cone tip
- Properties of particles
  - Density
  - Shape
  - Diameter
  - Particle size distribution
  - Rate of mass loading
- Properties of gas
  - Gas velocity at the inlet
  - Density
  - Viscosity
  - Temperature
  - Pressure at the inlet
- Other factors
  - Wall roughness
  - Eccentricity of vortex finder

2.5 The Computational Fluid Dynamics Approach for Cyclone Gas-Solid Flow Simulation

Computational modeling of fluid dynamic applications has been increased with the advancement of computer processing power and memory capacity during the last decades. In Computational Fluid Dynamics (CFD), partial differential equations that define the fluid flow are approximately transformed into the algebraic equations.

Better solutions could be obtained by solving these algebraic equations iteratively using advanced computers. Furthermore, verification of these models is necessary before utilizing for flow prediction of equipment optimizations.

One of the leading CFD simulation of cyclone was performed by Boysan et al [11]. They concluded that standard k -ϵ model is not sufficient to predict swilling flow in a cyclone as it leads to excessive turbulence viscosities and unlikely tangential velocities. Their model was solved in an axisymmetric Eulerian framework to reduce the computational power.

Since then many investigations have been carried out to predict gas-solid flow field and efficiency of cyclone separators. Bernard et al [12] have simulated a cyclone operating at high temperatures using Algebraic Stress Model (ASM). Using the same model, the grade efficiency curve of Stairmand cyclone was predicted by Hoffmann et al [13].

Hoekstra et al [14] have simulated the Stairmand high efficiency cyclone employing Reynolds Average Stress Model (RANS) and LES, and they have compared the models with the results which were obtained using Lessor Dropler Anemometry (LDA). Later on, many researchers have used his LDA measurements to verify their gas field of cyclone models.

Zhou and Soo [15] have simulated the cyclone using k -ϵ model and compared with their LDA measurements. Combined vortex of cyclone was closely predicted with the k -ϵ model.

B.Wang et al [16] have investigated the gas-solid flow of Lapple cyclone using Reynolds Stress Model (RSM). The predictions were in good agreement with measured results by same authors. Lagrangian model has been utilized to forecast particle trajectories and collection efficiency.

N. Fathizadeh and A. Mohebbi [17] have investigated effectiveness of removing black powder particles from natural gas. They have modeled and performed system optimization analysis on Stairmand high efficiency cyclone using Large Eddy Simulation (LES). The simulation result has revealed that the increase of gas flow up to design value enhances the collection efficiency.

3 MATHEMATICAL MODEL

3.1 The Governing Equations for the Gas Phase

All laminar and turbulent fluid flows are governed by the conservation laws of physics. Those conservation laws are;

- mass of a fluid is conserved

- rate of momentum change of a fluid particle, equals to the sum of forces acting on it (Newton's second law)

- rate of energy changing of a fluid particle, equals to the sum of rate of heat addition and rate of work done on it a fluid particle (First law of thermodynamics)

These laws on fluid flow can be represented by Navier-Stokes equations as follows [18].

Mass conservation equation for a compressible gas which is flowing in unsteady state turbulent flow is given below. This is also known as continuity equation.

$$\frac{\partial \rho}{\partial t} + div(\rho U) = 0 \qquad (3.1)$$

Where,

U = three dimensional mean velocity of flow

ρ = mean density of gas

For turbulence flow, mean velocity component and fluctuating velocity components could be written as follows.

$u = U + u'; u = U + u'; v = V + v'; w = W + w'$

$U = U + V + W;$

$u' = u' + v' + w';$

Where,

u = three dimensional velocity

u' = three dimensional instantaneous fluctuating velocity component

Reynolds equations

Momentum equation along 'x' axis;

$$\frac{\partial(\rho U)}{\partial t} + div(\rho U U) = -\frac{\partial P}{\partial x} + div(\mu \ grad \ U) + \left[-\frac{\partial(\rho \overline{u'^2})}{\partial x} - \frac{\partial(\rho \overline{u'v'})}{\partial y} - \frac{\partial(\rho \overline{u'w'})}{\partial z}\right] + S_{Mx}$$

(3.2)

Momentum equation along 'y' axis;

$$\frac{\partial(\rho V)}{\partial t} + div(\rho V U) = -\frac{\partial P}{\partial y} + div(\mu \ grad \ V) + \left[-\frac{\partial(\rho \overline{u'v'})}{\partial x} - \frac{\partial(\rho \overline{v'^2})}{\partial y} - \frac{\partial(\rho \overline{v'w'})}{\partial z}\right] + S_{My}$$

(3.3)

Momentum equation along 'z' axis;

$$\frac{\partial(\rho W)}{\partial t} + div(\rho W U) = -\frac{\partial P}{\partial z} + div(\mu \ grad \ W) + \left[-\frac{\partial(\rho \overline{u'w'})}{\partial x} - \frac{\partial(\rho \overline{v'w'})}{\partial y} - \frac{\partial(\rho \overline{w'^2})}{\partial z}\right] + S_{Mz}$$

(3.4)

Scalar transport equation;

$$\frac{\partial(\rho \Phi)}{\partial t} + div(\rho \Phi U) = div(\Gamma_\Phi \ grad \ \Phi) + \left[-\frac{\partial(\rho \overline{u'\varphi'})}{\partial x} - \frac{\partial(\rho \overline{v'\varphi'})}{\partial y} - \frac{\partial(\rho \overline{w'\varphi'})}{\partial z}\right] + S_\Phi$$

(3.5)

Where,

φ = a property of a flow

Φ = the mean of the property φ

Navier-Stokes equations could be solved using three main approaches. They are large eddy simulation (LES); Reynolds average Navior Stokes approach (RNAS) and direct numerical simulation (DNS).

Direct numerical simulation approach is applied to solve all equations that produce accurate results. However it is not practical to use DNS with present computer capacities, since it requires a very fine mesh. Computational cost is proportional to Re^3.

3.1.1 Reynolds Averaged Navier Stokes (RANS) Approach

Turbulent flow analysis approach in RANS simulation divides flow into two parts; a mean component and a fluctuating component. This is known as Reynolds decomposition.

$u_i u_j$ terms are called Reynolds stress tensor. They denote correlation between fluctuating velocities and add more variables to the Navior Stokes equations. Closure models are used to define these terms, in terms of mean quantities. These closure models are called turbulence models.

The standard k-ε model

One of the well-known turbulent model is k-ε model which is used for simulation of gas flow in cyclone. It is a two equation model and it solves two additional transport equations related to turbulent kinematic energy (k) and its rate of dissipation (ε).

The standard k-ε model equations by Launder and Spalding [19].

$$\mu_t = \rho C_\mu \frac{k^2}{\epsilon} \tag{3.6}$$

Where,

μ_t = eddy (turbulent) viscosity

C_μ = dimensionless constants

k = turbulent kinetic energy

ε = dissipation of turbulent kinetic energy

Standard transport equations for k and ε;

$$\frac{\partial(\rho k)}{\partial t} + div(\rho k U) = div\left(\frac{\mu_t}{\sigma_k} \ grad \ k\right) + 2\mu_t E_{ij}.E_{ij} - \rho\varepsilon \tag{3.7}$$

$$\frac{\partial(\rho \varepsilon)}{\partial t} + div(\rho \varepsilon U) = div\left(\frac{\mu_t}{\sigma_\varepsilon} \ grad \ \varepsilon\right) + 2C_{1\varepsilon}\frac{\varepsilon}{k}2\mu_t E_{ij}.E_{ij} - \rho C_{2\varepsilon}\frac{\varepsilon^2}{k} \tag{3.8}$$

Five dimensionless adjustable constants in the above equations are C_μ =0.09, $\sigma_k = 1.0$, $\sigma_\varepsilon = 1.3$, $C_{1\varepsilon} = 1.44$ and $C_{2\varepsilon} = 1.92$. These values could be changed to obtain best fitted turbulence model for given application.

18

Boussinesq et al [20] have proposed equation to link Reynolds stress terms in to mean flow rates of decomposition. Following equation is used in k-ϵ model to calculate Reynolds stress.

$$-\rho\overline{u_i'u_j'} = \mu_t \left(\frac{\partial U_i}{\partial x_i} + \frac{\partial U_j}{\partial x_j}\right) - \frac{2}{3}\rho k\delta_{ij} = 2\mu_t E_{ij} - \frac{2}{3}\rho k\delta_{ij} \qquad (3.9)$$

Where,

δ_{ij} = Kronecker delta

δ_{ij} equals to 1, if i=j and equal to zero when i≠j.

3.2 Modeling the Particle Phase

Lagrangian and Eularian approach could be used to model particulate phase in the gas flow. Eularian approach is only applicable to the high concentration flows, where it is assumed that the flow is continuous. Lagrangian approach is suitable for diluted concentrations, where it can be used to model particles behavior individually or as parcels. Each property of a particle is a function of its position and time. Writing momentum and energy conservation laws of a particle is termed as Lagrangian approach.

Multiphase Particle in Cell (MPPIC) method [21] is used for the particle modeling, which is an in-built collisional model in OpenFOAM. Particle interactions with other particles are represented by models, which applies mean values calculated on the Eularian mesh.

3.2.1 Governing equations of Multiphase Particle in Cell (MPPIC) method

Probability distribution function (PDF), $\emptyset$ is used to describe particle phase.

$$\frac{\partial \emptyset}{\partial t} + \nabla.(\emptyset u_p) + \nabla_{u_p}.(\emptyset A) = 0 \qquad (3.12)$$

Where,

A = particle acceleration, m/s^2

u_p = particle velocity, m/s

Particle phase numerical solution was obtained by dividing distribution into parcels. That is used to represent finite number of particles with known properties such as density, velocity, and position. Use of parcels has significantly reduced the

19

computational load. Local properties could be obtained by integrating probability distribution function (Ø)

Particle volume fraction;

$$\theta_p = \int\int\int \emptyset\Omega_p d\Omega_p \, d\rho_p du_p \qquad (3.103)$$

Average density of particles;

$$\overline{\theta_p\rho_p} = \int\int\int \emptyset\Omega_p\rho_p d\Omega_p \, d\rho_p du_p \qquad (3.14)$$

Mean velocity of particles;

$$\overline{u_p} = \frac{1}{\overline{\theta_p\rho_p}}\int\int\int \emptyset\Omega_p\rho_p u_p d\Omega_p \, d\rho_p du_p \qquad (3.15)$$

Where,

Ω_p = particle volume at position x and time t, m³

Paricle pahse and gas phase coupled using particle acceleration term as follows.

$$A = D_p(u_g - u_p) - \frac{\nabla p}{\rho_p} + g - \frac{\nabla\tau}{\theta_p\rho_p} \qquad (3.16)$$

Where,

D_p = diameter of the particle

τ = particle stress [22]

$$\tau = \frac{P_s\theta_p^\beta}{max[\theta_{cp}-\theta_p,\epsilon(1-\theta_p)]} \qquad (3.17)$$

Where,

θ_{cp} = close pack volume fraction

P_s, ϵ and β are constants

Particle phase and gas phase momentum exchange rate 'F' could be written as follows.

$$F = \int\int\int \emptyset\Omega_p\rho_p\left[D_p(u_g - u_p) - \frac{\nabla p}{\rho_p}\right] d\Omega_p d\rho_p du_p \qquad (3.11)$$

4 COMPUTATIONAL FLUID DYNAMIC MODEL (OPENFOAM)

4.1 Geometry and Mesh Preparations

For the computer simulation Lapple cyclone was selected since it is very common in the industry. And also verification data for Lapple cyclone could be found in the literature. Calculated dimension values are given in table. 4.1. Cyclone diameter (D) is 0.2 m.

Table 4.1 : Dimensions of Lapple cyclone

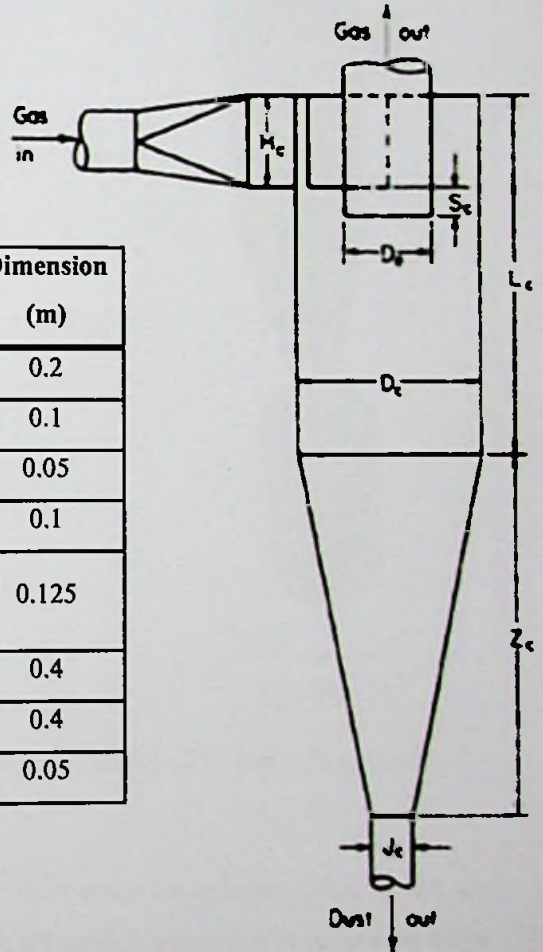| Item	Ratio	Dimension (m)
Diameter of body, D/D	1.0	0.2
Height of inlet, H_c/D	0.5	0.1
Width of inlet, B_c/D	0.25	0.05
Diameter of gas exit, D_e/D	0.5	0.1
Length of vortex finder, (H_c + S_c) /D	0.625	0.125
Length of body, L_c/D	2.0	0.4
Length of cone, Z_c/D	2.0	0.4
Diameter of dust outlet ,J_c/D	0.25	0.05

Figure 4.1: Lapple cyclone

Geometry of the cyclone is prepared using Blender® software[39]. Blender is an open source 3D content creation program, which is developed and maintained by a non-profit organization. Mesh generation was done by the OpenFOAM® pre prossecing facility. OpenFOAM has inbuilt mesh generation fasility. Three meshes were generated with containing 23,444, 52,236, and 272,340 hexahedron cells. However concidering time taken for solving very fine meshes and resanable accurate

results of medium size mesh, medium size mesh was use for the simulation. Furthermer B.Wang et al [16] have obtaied accurate results compared to test carried-out by himself with the use of mesh containg 45,750 cells for same geometry.
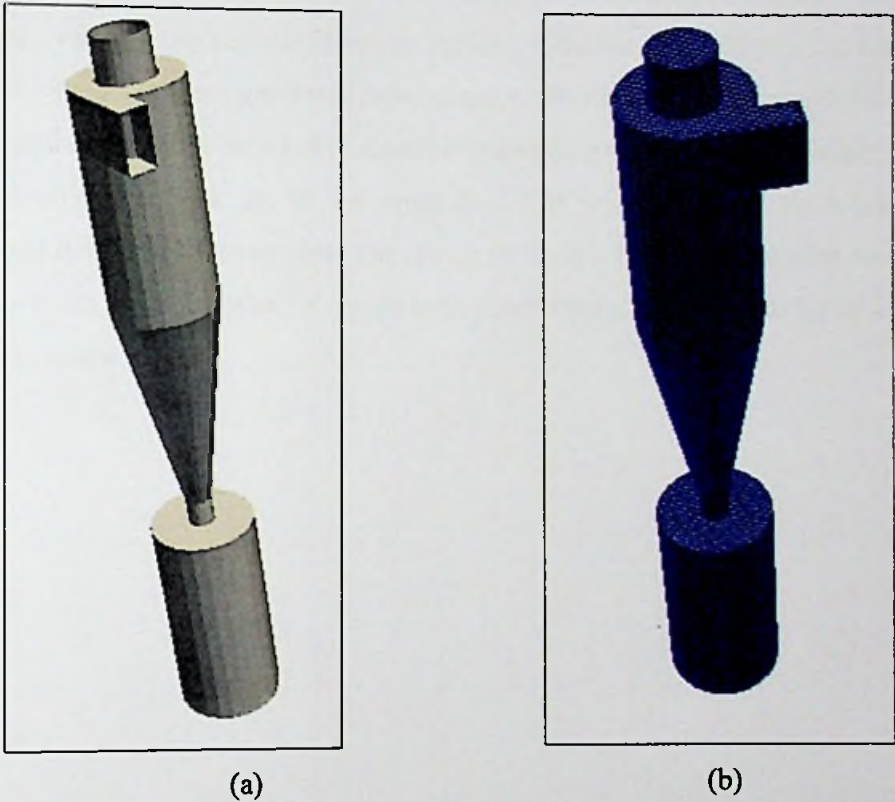

(a)   (b)

Figure 4.2 : 3D view of a) Cyclone geometry and b) CFD mesh of cyclone

4.2   Boundary conditions

Cyclone separator body was segregated into three main boundaries: inlet, outlet, and wall. Functions applied for boundaries of RANS models are given in following table.

Table 4.2 : Functions applied for boundaries of RANS

Applied Boundary Function	Boundary name		
	Inlet	Outlet	Wall
Velocity(u)	fixed value	calculated	fixed value (0, 0, 0)
Pressure(p)	calculated	fixed value (0)	calculated
Turbulent viscosity (nut)	calculated	calculated	wall model
kinetic energy (k)	fixed value	calculated	wall model
Rate of dissipation (epsilon)	fixed value	zero gradient	wall model

4.3   Particle injection models

4.3.1   Based model

This model was prepared according to the test experiments conducted by B.Wang et al [16]. Their experimental results were used to validate developed CFD models.

Both inlet gas velocity and particle injection velocity were set to be 20 m/s for the based model. Particles were generated from cement raw material grinding. Rosin-Rammler distribution could be used to describe particles generated from grinding. Characteristic diameter was set to be equal to 29.90 μm and the distribution parameter was 0.806. Solid mean flow rate was 0.03 kg/m^3. Density of cement raw material was taken as 3320 kg/m^3. Pressure at cyclone separator outlet was equal to the ambient pressure.

5 RESULTS AND DISCUSSION

5.1 RANS Simulation Results and Discussion

5.1.1 Overall flow pattern

RANS simulation has predicted the overall gas flow pattern as described in the literature. Gas flow enters the cyclone through the tangential inlet, where the gas flow is forced into a cyclic movement down the cyclone. At the bottom of cyclone, gas turns upwards and spirals up around the center axis and then exit through the vortex finder.
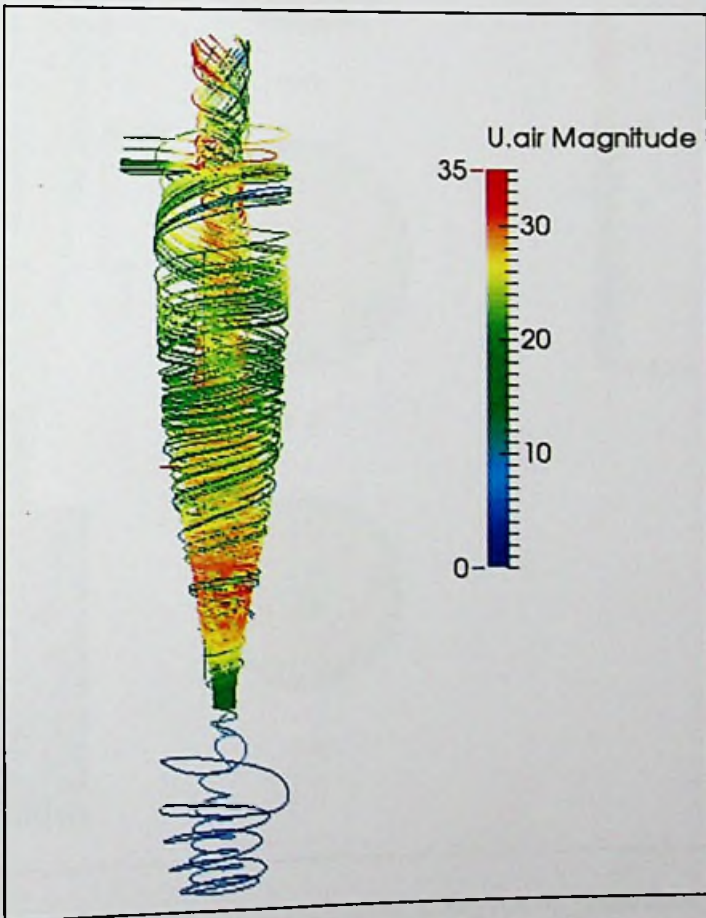

Figure 5.1 : Gas flow path generated by RANS simulation

Path of the gas flow inside the cyclone generated by RANS simulation is shown in the figure 5.1. Velocity variation of gas flow is indicated by a color scheme. Inlet gas velocity was kept at 20 m/s.

5.1.2 Gas velocity profile

Figure 5.2 shows the detail velocity distribution of the gas flow inside the cyclone. Cross sections of different levels clearly illustrate the magnitude of the velocity at respective locations.
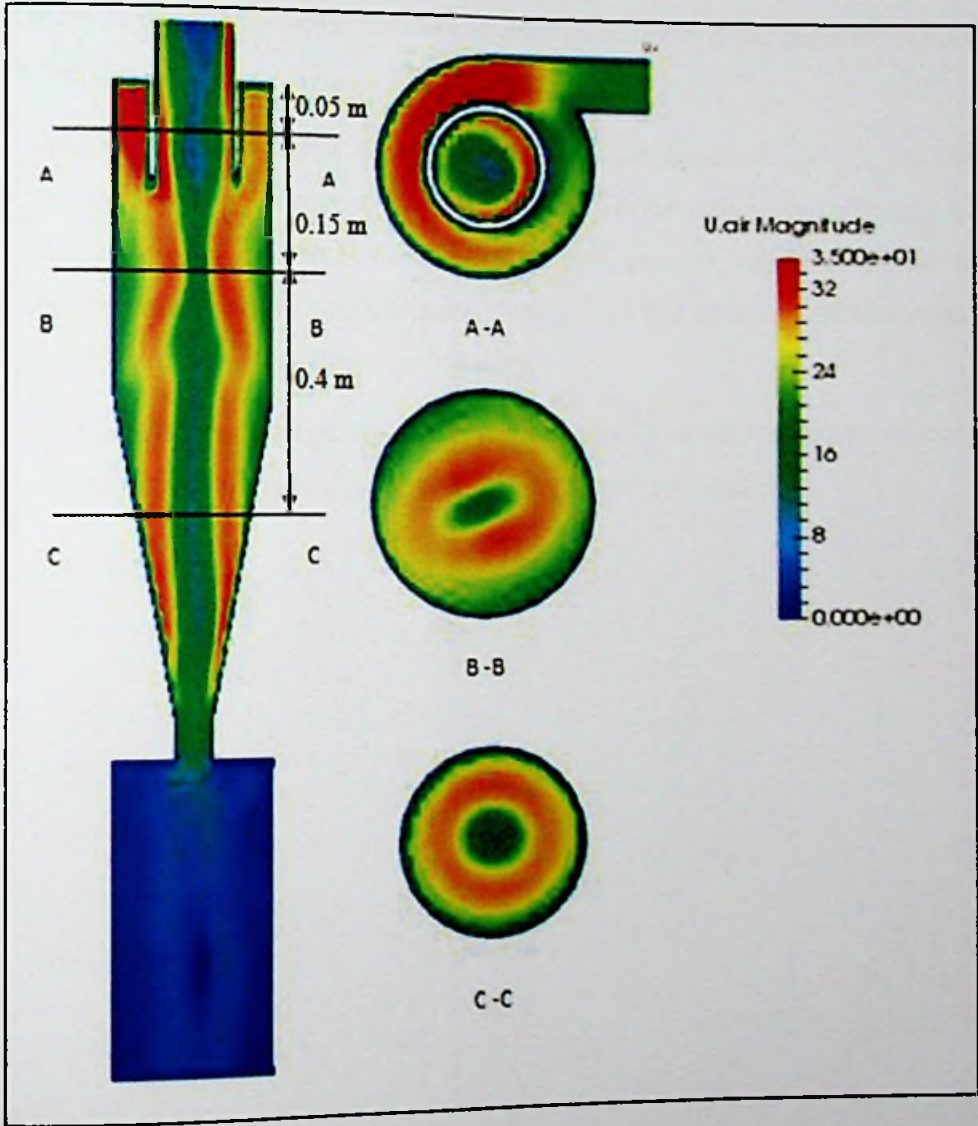

Figure 5.2: Velocity profile of cyclone obtained using RANS simulation (at 20 m/s inlet gas velocity

Figure 5.2 shows the variation of magnitude of gas flow velocity inside the cyclone. According to the section A-A flow velocity was rapidly increased just after the entering to the cyclone. Maximum velocity recorded in that area was about 35 m/s. A low velocity zone has created at the right side of section A-A. From there, a part of

the gas flow is added to the inlet-flow and the rest is directed downwards creating a spiral movement. As a part of the flow is added to the inlet-flow, the high velocity zone has been created at the left side of section A-A.

According to the literature gas flow of the inlet area could be accelerated up to 1.5 to 2 times of the inlet velocity. This fact is clearly visualized in the cross section A-A of cyclone.

Considering the area below the vortex finder, the magnitude of velocity has become comparatively small closer to the vertical axis and the wall of the cyclone. A high velocity zone has created in between above two areas, at a distance similar to the radius of vortex finder, from the center. Velocity of that area reached up to about 30 m/s, which is 1.5 times of inlet gas velocity.

As the gas moves out from the vortex finder, velocity of gas has again reduced. Gas flow velocity at the particulate collecting bin has also reduced.

5.1.3 Tangential gas velocity profile obtained using RANS model

Tangential gas velocity component of cyclone has increased along the radial direction from cyclone axis up to a distance equal to diameter of vortex finder, and there it obtained the highest value. From there on wards it reduces. Image of cyclone vertical cross section (figure 5.3) clearly indicates the areas where tangential velocity exceeds the inlet velocity.
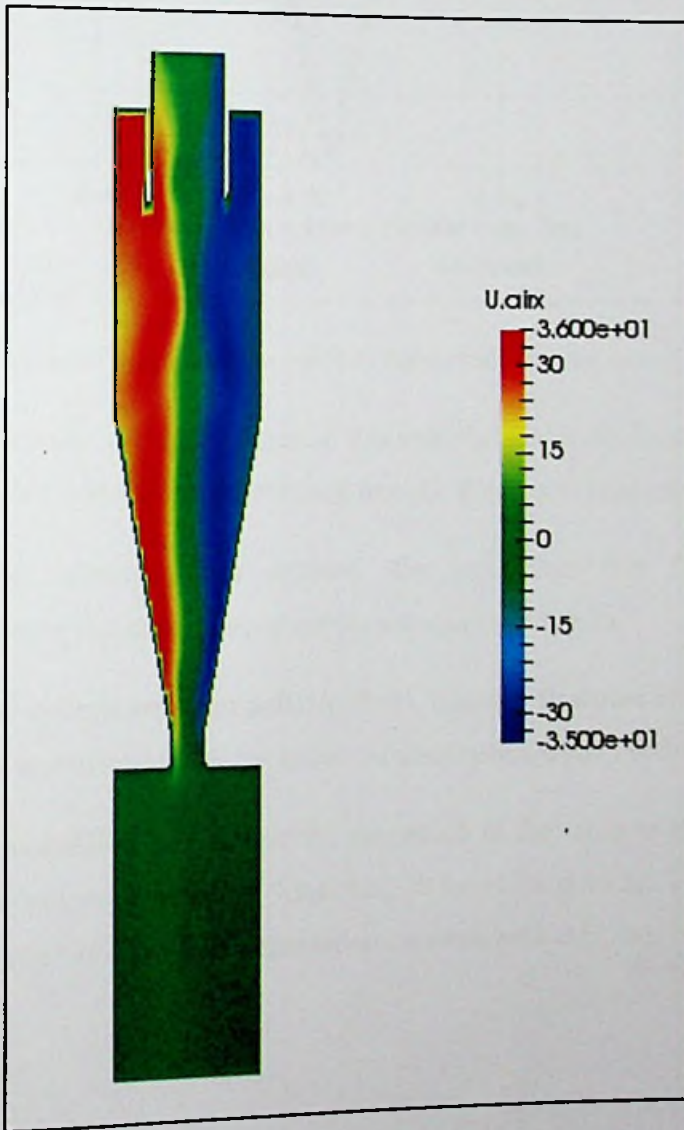

Figure 5.3: Tangential velocity profile of cyclone obtained using RANS simulation (at 20 m/s inlet gas velocity)
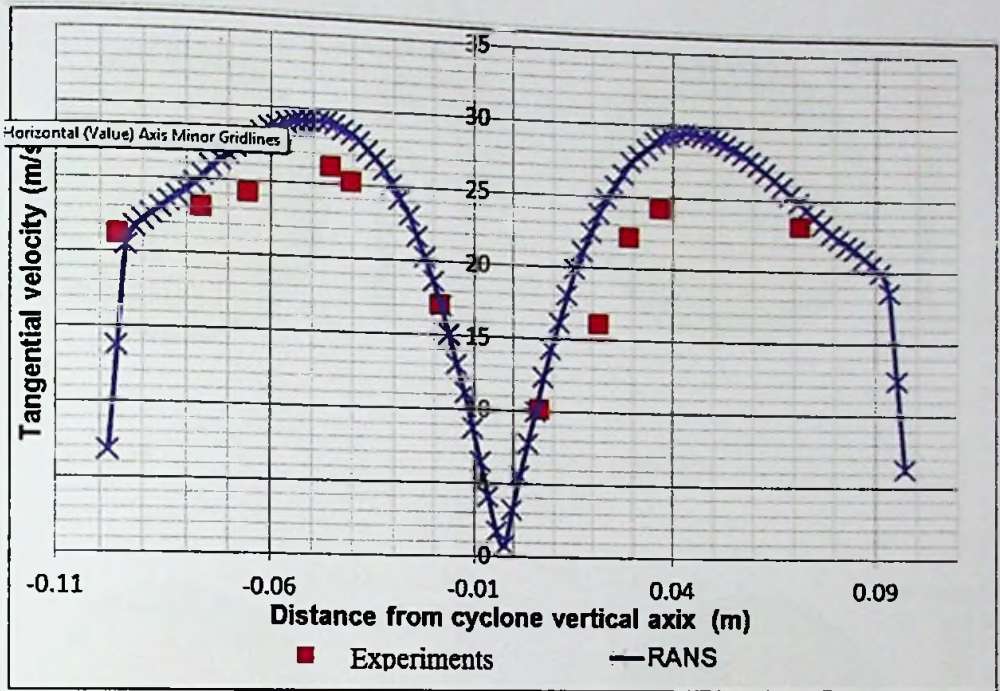
Figure 5.4 : Averaged tangential gas velocity compared with the experiments

Figure 5.4 illustrates averaged tangential gas velocity values obtained during stable simulation period with the results obtained from B. Wang et al [16] experiments.

Tangential gas velocity values obtained after more than fifty flushes of the simulation. During that time velocity profile patterns were similar.

Volume of the cyclone separator is 0.01675 m^3. Inlet gas flow rate at 20 m/s is 0.10 m^3. Therefore approximately six complete volume flushes happen within a second.

Figure 5.5 is visualized the gas velocity magnitude of the cross section B-B (refer figure 5.2) of cyclone separator at 9.5 s, 10s, 10.5s, 11s and 11.5s. This shows that cyclone separator velocity pattern orientation variation with the time.
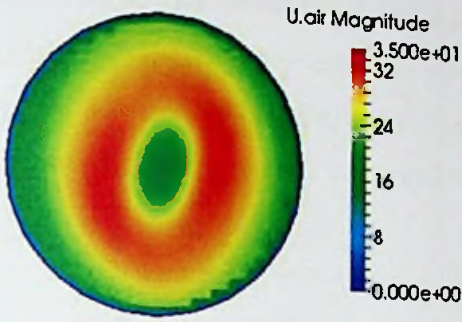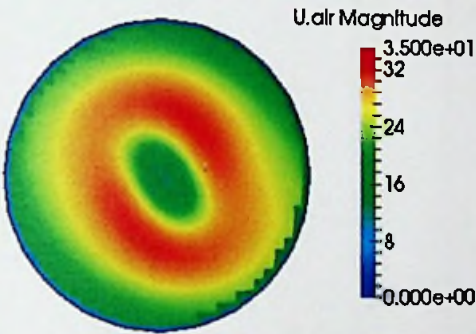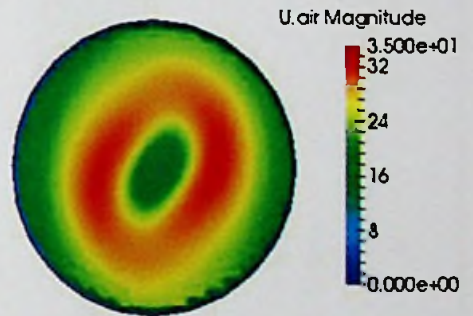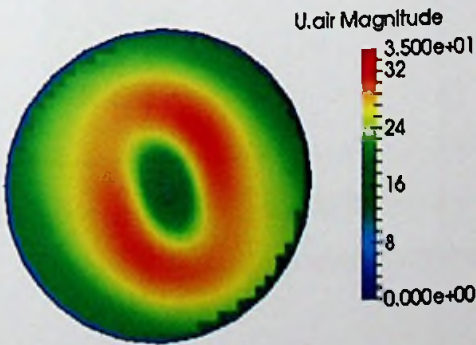
(a) 9.5s
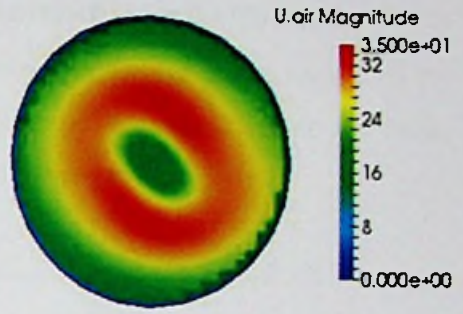
(b) 10s

(c) 10.5s

(d) 11 s

(d) 11.5 s
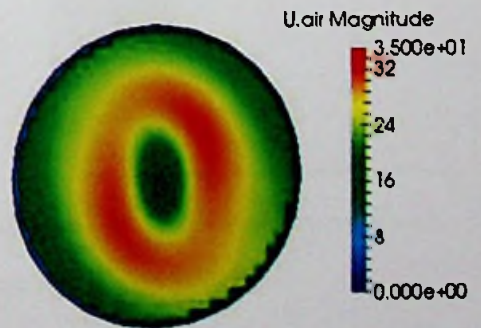
(e) 12 s

Figure 5.5 : Gas velocity magnitude pattern at different time instance of the cross section B-B (figure 5.2) of RANS simulation

5.1.4 Axial and radial gas velocity profiles obtained using RANS model

Axial gas velocity component of cyclone separator is upward in the middle of the cyclone separator along the vertical axis and it moves downward near to the walls. The radial velocity is small compared to tangential velocities.
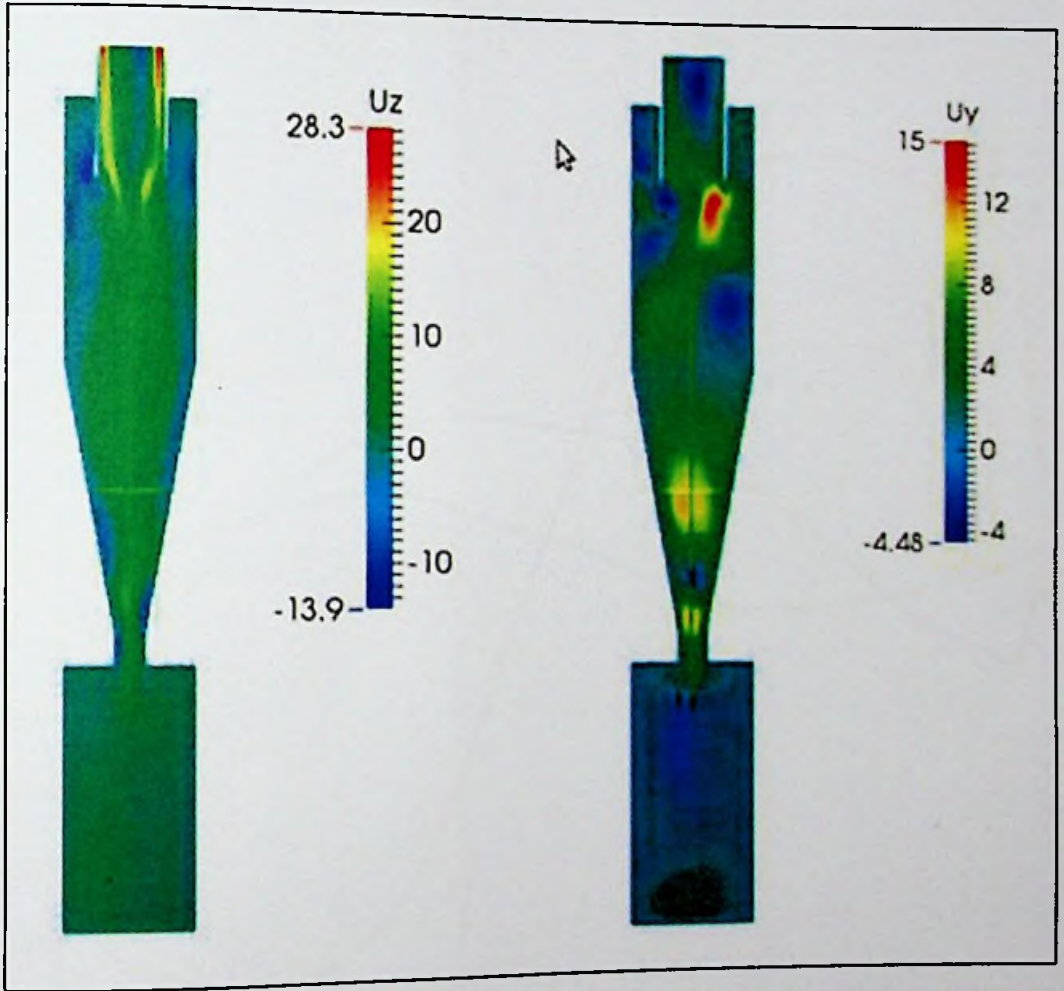
Figure 5.6: Axial (Left side figure) and Radial (Right side figure) velocity profile of cyclone separator obtained using RANS simulation

Figure 5.7 shows axial, radial and tangential gas velocity variation along the radius of the cyclone. Axial and radial gas velocities are comparatively low in magnitude compare to tangential velocity. Therefor tangential velocity is the dominant velocity which creates the pressure distribution pattern in the cyclone. Velocities at the wall reduce rapidly due to boundary layer effect.

Figure 5.7: Axial(U_z), radial(U_y) and tangential (U_x) gas velocities at the cross section B-B (figure 5.2) of RANS simulation

5.1.5 Pressure distribution

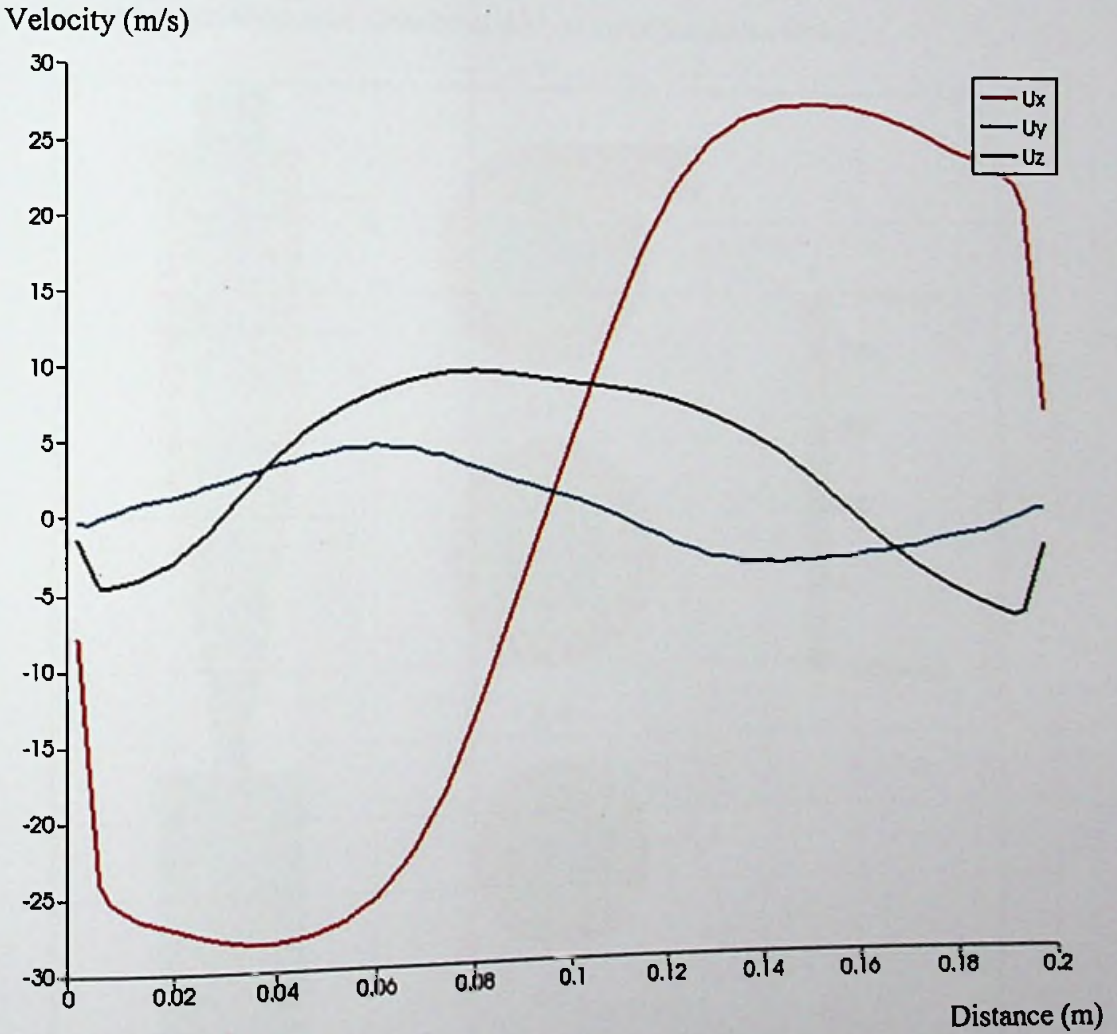Figure 5.6 shows the pressure distribution pattern obtained from the model. A negative pressure zone has created at the center, which is the lowest pressure inside the cyclone. This negative pressure zone has appeared throughout the vertical axis of the cyclone. A high pressure zone is created near to the walls. Furthermore pressure at the right side of the inlet area is high (cross section A-A). This make high pressure zone and low pressure zone close by at the bottom of the vortex finder.
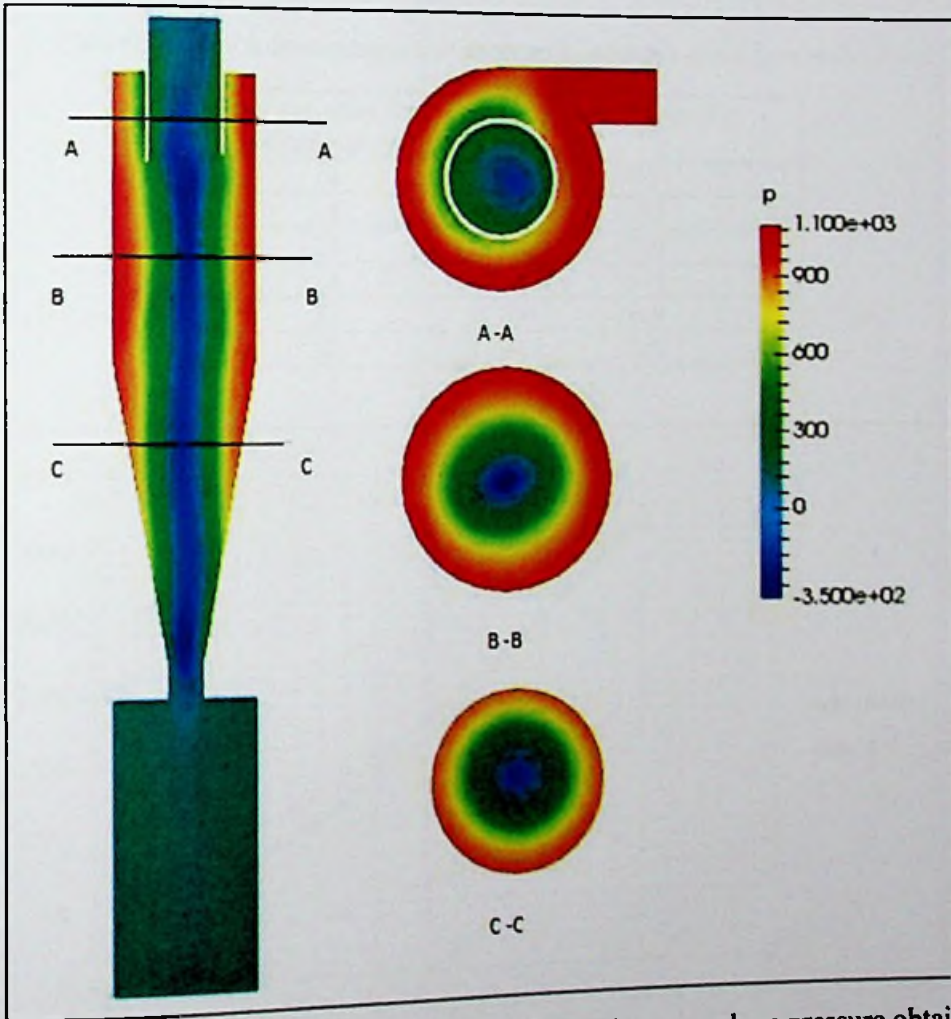

Figure 5.8 : Pressure profile of cyclone relative to the atmosphere pressure obtain using RANS simulation

Due to this occurrence, there is a possibility of short-circuiting part of the gas solid flow without moving along its conventional spiral path. This results the re-contamination of the purified gas flow.

Pressure distribution pattern of the cyclone simulation illustrates the pattern suggested by Ter Linden [4], which is explained in the section 2.3.3.

5.1.6 Pressure drop

Effect of gas-solid inlet velocity on the cyclone pressure drop was analyzed using six simulations. Particles were injected to the cyclone in a same velocity as the gas velocity. Except gas-solid flow velocities, all other parameters were maintained constant. Solid mean flow rate was 0.03 kg/m³.

Table 5.1 : Cyclone pressure variation with inlet gas-solid flow velocity

Inlet gas-solid flow velocity (m/s)	Pressure drop (Pa)
15	792
18	1092
20	1380
23	1809
25	2220
30	3216
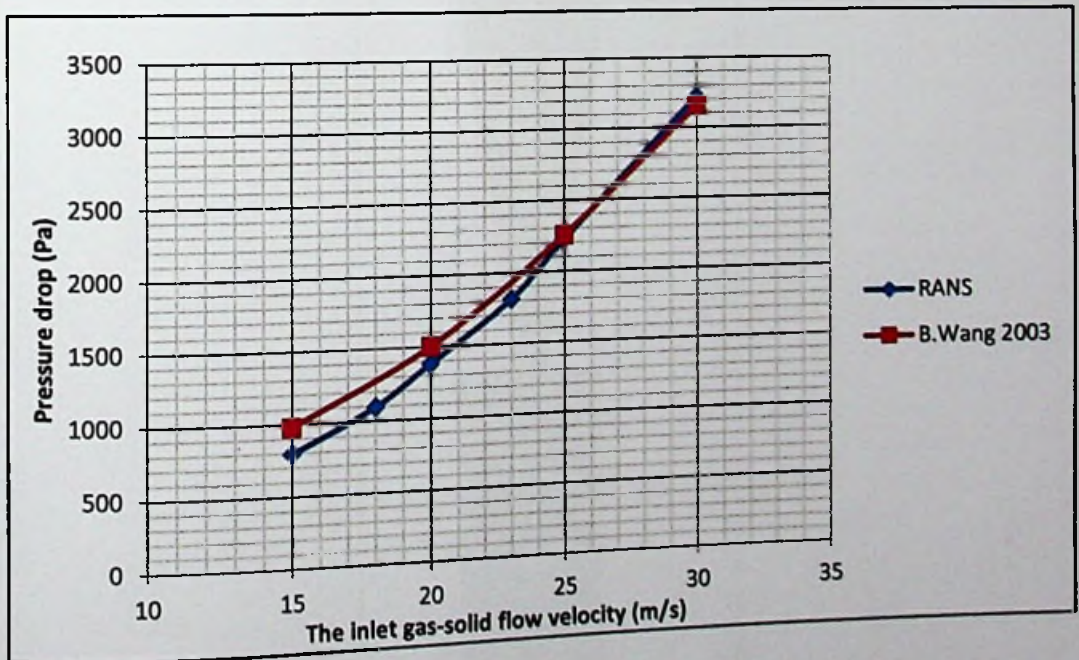
Figure 5.9 : Variation of cyclone pressure drop with inlet gas-solid flow velocity Simulation results of RANS simulation closely matches with the test results of B. Wang et al [16].

33

5.1.7　Collection efficiency of cyclone

5.1.7.1　Effect of operational parameters variation on performance of cyclone

While maintaining all other parameters described in the base model, each parameter was varied to obtain optimum collection efficiency of the cyclone.

Verification of the RNAS model was done by comparing the results of the model obtained for gas-solid velocity vs. collection efficiency with test results of B. Wang et al [16].

Figure 5.10: Particle simulation of Lapple cyclone obtain using RANS simulation

Effect of Inlet gas-solid velocity variation

Table 5.2: Variation of collection efficiency with inlet gas-solid flow velocity

Inlet gas-solid flow velocity (m/s)	Collection efficiency %
15	92.5
18	95.4
20	96.4
23	96.4
25	96.1
30	94.7
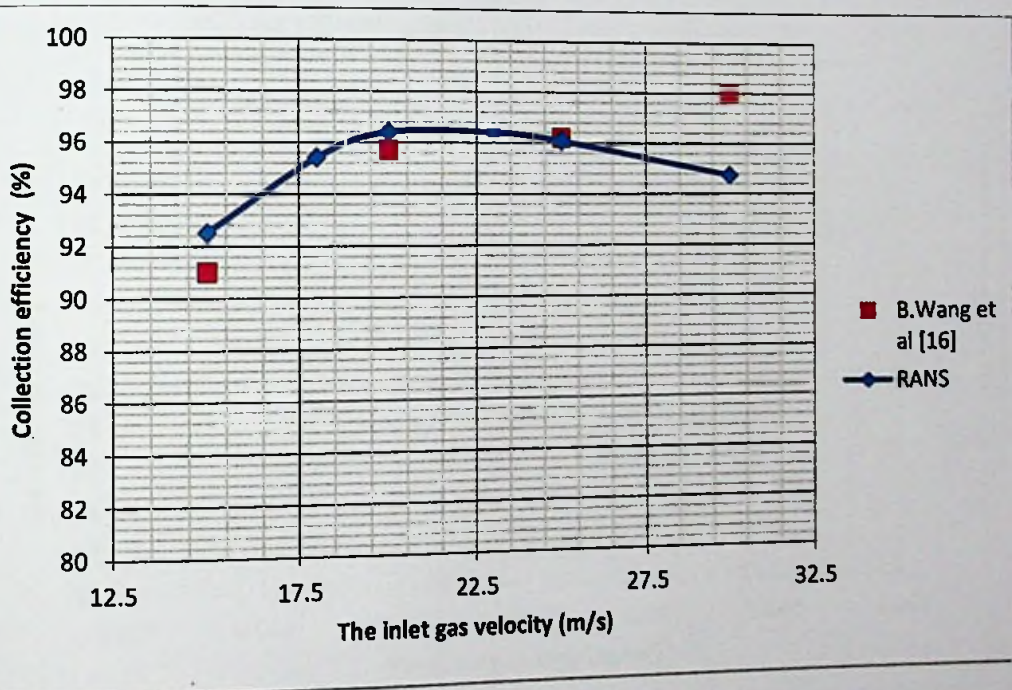
Figure 5.11 : Cyclone collection efficiency variation with inlet gas-solid flow velocity

According to the figure 5.8, results obtained from the model are approximately similar to the test results at low velocities below 25 m/s. The $\chi 2$ statistic for the data for analytical and test results is 98.67. However result obtained at 30 m/s shows deviation from the experimental results.

Collection efficiency has increased with the increasing velocity and has recorded the maximum efficiency at 20 m/s. Then the efficiency is slightly reduced with

increasing inlet gas-solid velocity. Therefore optimum inlet gas-solid velocity could be taken as 20 m/s.

Effect of particulate loading rate variation

Table 5.3: Variation of collection efficiency with particulate loading rate

Particle loading rate	Collection efficiency %
750 mg/s (0.007kg/m³)	89.6
1518 mg/s (0.015kg/m³)	92.0
3000 mg/s (0.030kg/m³)	96.4
6000 mg/s (0.060kg/m³)	97.2

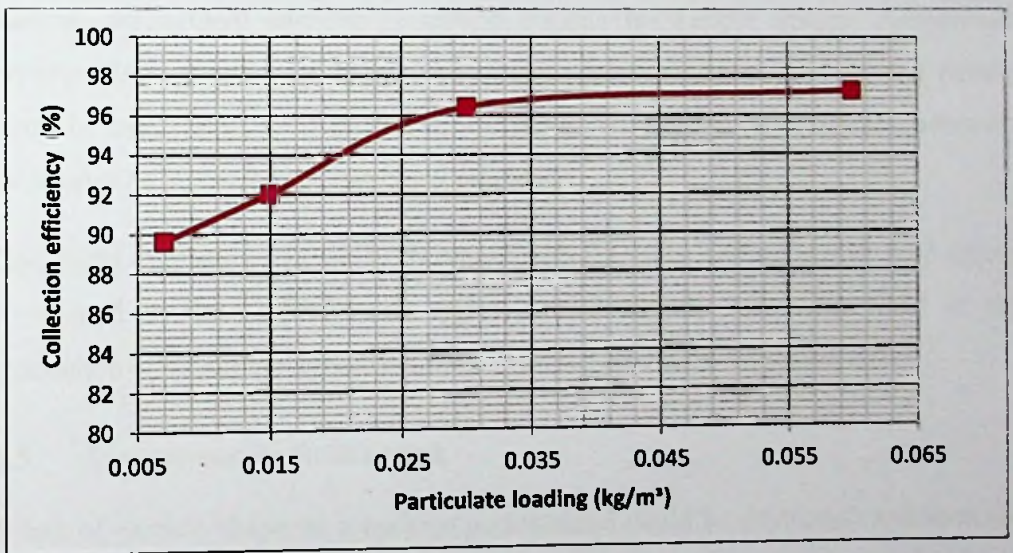

Figure 5.12 : Cyclone collection efficiency variation with inlet particulate loading

Figure 5.9 shows a rapid increase of collection efficiency with the increase of particulate (solid) loading rate up to about 0.03 kg/m³. Then the efficiency slightly increases with the increase of particulate loading rate. Therefore optimum particulate loading rate could be taken as range 0.045 – 0.06 kg/m³.

6   CONCLUSION

6.1   Gas flow field simulation

It can be concluded that RANS model reasonably predict the gas-solid flow pattern of the cyclone. Pressure drop and collection efficiency of cyclone with respect to different inlet gas velocities were well fitted to the test results. The χ^2 statistic for the data for analytical and test results of collection efficiency is 98.67. For these comparisons experimental results given in [16] were used.

6.2   Particle collection and optimization

Collection efficiency of cyclone was increasing with the inlet gas velocity up to around 20 m/s and beyond that it was slightly reducing. Optimum cyclone inlet velocity for cement particles is around 20 m/s for Lapple design. Furthermore pressure drop variation of the cyclone with the inlet velocity was increasing rapidly with the inlet velocity. Therefore depending on the separation efficiency necessity inlet velocity below 20 m/s can be recommend.

Collection efficiency of cyclone increased with the mass loading. At the 0.03 kg/m3 it reached to the highest value and remained slightly increasing trend in the simulation. This slight increase could be occurred due to the sweeping effect.

6.3   Suggestions for future work

Effect of particle shape on a cyclone performance could be developed and used for cyclone parameter optimization for different shapes. In this research it has been assumed that all particles are in spherical shape.

Cyclone fine particle collection efficiency could be analyzed and optimized by injecting water droplets.

REFERENCE LIST

1. J. M. Coulson & J. F. Richardson, "Equipment Selection, Specification and Design," in *Chemical Engineering Design*, 4th ed. Oxford, UK, 2003, ch.10, pp. 450-458.

2. C. D. Cooper, F. H. Alley, "Cyclones," in *Air pollution control- a design approach*, 2nd ed. Waveland, 1994, ch.4, pp. 1127-147.

3. R. H. Perry and D. W. Green, " Gas-Solid Seperations," in *Perry's Chemical Engineers'Handbook*, 7th ed. McGraw-Hill, 1997, ch.17, pp. 17.23-17.31.

4. A. J. Ter Linden, "Cyclone dust collectors," Proc. Inst. Mech. Eng.160, 1949.

5. C. B. Shepherd, C. E Lapple, "Flow pattern and pressure drop in cyclone dust collectors", 1939.

6. J. Hoekstra, J. J. Derksen, and H. E. A. Van Den, "An experimental and numerical study of turbulent swirling flow in gas cyclones," *Chemical Engineering Science*, 1999.

7. R. M. Alexander, "Fundamentals of Cyclone Design and Operation", Proc. Aus. Inst. Min. Met. 1949, pp.152-228.

8. W. Licht, " Control of Particles by Mechanical Collectors", in *Handbook of Air pollution Technology*, S. Calvert and H.m. Englund, Eds, New York: Wiley,1984, cp.13.

9. K. Woodard, "Stationary Source Control Techniques Document for Fine Particulate Matter," U.S. Environmental Protection Agency, 1998, PP-5.1-5.1-34

10. Air & Waste Management Association, "Air Pollution Engineering Manual," Van Nostrand Reinhold, New York. NY, 1992.

11. Boysan, W.H. Ayer, and J.Swithenbank, "Fundamental mathematical-modeling approach to cyclone design," Transaction of Institute Chemical Engineers, 1982.

12. J.G. Bernard, J. Andries, and B.Scarlett, "Cyclone research for application at high temperatures and pressures," in *1st European Symposium Separation of Particles from Gases*, 1989.

13. A.C. Hoffmann, M. de Groot and A. Hospers, "The effect of the dust collection system on the flow pattern and separation efficiency of a gas cyclone," 1996.

14. J. Hoekstra, J. J. Derksen, and Van de Akker, "Gas flow field and collection efficiency of cyclone separators," 2000.

15. L.X. Zhou and S. L. Soo, "Gas-solid flow and collection of solid in a cyclone separator," 1990.

16. B. Wang, D.L. Xu, K.W. Chu, and A.B. Yu, "Numerical study of gas-solid flow in a cyclone separator," in *Third International Conference on CFD in the Minerals and Process Industry*, Australia, 2003.

17. N. Fathizadeh, A. Mohebbi, S. Soltaninejad and M. Iranmanesh, "Design and simulation of high pressure cyclones for a gas city gate station using semi-empirical models, genetic algorithm and computational fluid dynamics," *Journal of Natural Gas Science and Engineering*, 2015.

18. K. Versteeg and W. Malalasekera, *An Introduction to Computational Fluid Dynamics*, 2nd ed. Harlo: Pearson Education Limited, 2007.

19. E. Launder and D. B. Spalding, "The numerical computation of turbulent flows," *Computer Methods in Applied Mechanics and Engineering*, 1974.

20. J. V. Boussinesq, "Essay on The Theory of Running Water," *Memories Presented by Various Scholars has Achedamy Sciences XXIII*, 1877, IEEE Transl.

21. M. J. Andrews and P. J. O'Rourke, "The Multiple Particle-In-Cell Method for Dense particle flows," 1996.

22. M Sinder, "An Incompressible Three Dimensional Multiple Particle-In-Cell Method for Dense particle flows," *Journal of Computational Physics*, 2001.

23. L. Iozia and D. Leith, "Effect of cyclone dimensions on gas flow pattern and collection efficiency," in *Aerosol Science and Technology*, 1989.

24. *OpenFOAM user guide*, Version 2.2.0., The open source CFD toolbox, 2013.

25. *Programmer's guide*, Version 2.1.1., The open source CFD toolbox, 2012.

26. J. Smagorinski, "General circulation experiments with the primitive equations", 1963.

27. V. Singh et al, "Simulation of gas-solid flow and design modifications of cement plant cyclones", in *Fifth International Conference on CFD in the Process Industries*, CSIRO, Melbourne, Australia, 2006.

28. D. Papoulias, S. Lob, "Advances in cfd modeling of multiphase flows in cyclone separators", 2015.

29. D. B. Dias, M. Mori and W. P. Martignoni, "Boundary condition effects in CFD cyclone simulations"

30. K.W. Chu et al, "CFD–DEM simulation of the gas–solid flow in a cyclone separator" *Chemical Engineering Science*, vol. 66, pp. 834-847, 2011.

31. P. A. Funk, S. Ed Hughs and G. A. Holt, "Engineering and ginning- Entrance velocity optimization for modified dust cyclones", The *Journal of Cotton Science* vol.4, pp.178-182, 2000.

32. G. Gronald and J.J. Derksen, "Simulating turbulent swirling flow in a gas cyclone: a comparison of various modeling approaches", 2010.

33. J. J. Derksen, "LES for swirling flow in separation devices"

34. J. J. Derksen, "Separation performance predictions of a stairmand high-efficiency cyclone", *AIChE Journal*, Vol. 49, No. 6, pp. 1359-1376, 2003.

35. A. H. B. Badarisman, *Modeling of high efficiency miniature aerocyclone*, B.Sc. thesis, Univ. of Malayasia Phang, Malayasia, 2010.

36. E. A. R. Stendal, *Multiphase flows in cyclone separators: modeling the classification and drying of solid particles using CFD*, M.Sc. thesis, Chalmers Univ. of technology, Gothenburg, Sweden, 2013.

37. Liang Ma et al, "CFD simulation study on particle arrangements at the entrance to a swirling flow field for improving the separation efficiency of cyclones", *Aerosol and Air Quality Research*, vol.15, pp. 2456–2465, 2015.

38. L. Wang, *Theoretical study of cyclone design*, PhD Dissertation, Texas A&M Univ., 2004.

39. Wikipedia. (2015, December 15). *Blender(software)* [Online] Available: https://en.wekipedia.org/wiki/Blender_(software)

APPENDIX I

Rosin-Rammler particle distribution

Rosin & Rammler (1933) particle size distributions model is widely used to describe particle size distribution of grinded materials.

$$f(x; P_{80}, m) = \begin{cases} 1 - e^{ln(0.2)\left(\frac{x}{P_{80}}\right)^m} & x \geq 0, \\ 0 & x < 0, \end{cases}$$

Where,

x =Particle size

P_{80} = 80th percentile of the particle size distribution

m =Parameter describing the spread of the distribution

The inverse distribution is given by:

$$f(F; P_{80}, m) = \begin{cases} P_{80} \sqrt[m]{\frac{ln(1-F)}{ln(0.2)}} & F > 0, \\ 0 & F \leq 0, \end{cases}$$

Where,

F= Mass fraction

Parameter estimation

The parameters of the Rosin–Rammler distribution could be resolute by refactoring the distribution function to the form

$$\ln\left(-\ln\left(1 - F\right)\right) = m \ln(x) + \ln\left(\frac{-\ln(0.2)}{(P_{80})^m}\right)$$

Hence the slope of the line in a plot of

$\ln\left(-\ln\left(1-F\right)\right)$ versus $\ln(x)$ yields the parameter m and P_{80} is determined

$$P_{80} = \left(\frac{-\ln(0.2)}{e^{intercept}}\right)^{\frac{1}{m}}$$

by substitution into